Study the Effect of Trailing Edge Flap Deflection on Horizontal Axis Wind Turbine Performance Using Computational Investigation

Mohamed B. Farghaly *‡, E. S. Abdelghany **

* Mechanical Engineering Department, Faculty of Engineering, Fayoum University, 63514, Fayoum, Egypt

** Mechanical Engineering Department, Faculty of Engineering, Albaha University KSA, on Leave from Institute of Aviation Engineering and Technology, Egypt

(mbs12@fayoum.edu.eg , bader_pilot@yahoo.com; Eslam_said312002@yahoo.com, eslam@bue.edu.sa)

‡ Corresponding Author; Mohamed B. Farghaly, Mechanical Engineering Department, Faculty of Engineering, Fayoum University, keman Faras Street, Fayoum 63514, Egypt, Tel: +20 100 820 0258, mbs12@fayoum.edu.eg, bader_pilot@yahoo.com

Received: 12.09.2022 Accepted: 22.10.2022

Abstract- Improving the aerodynamic performance of wind turbine blade is considered one of the most significant factors to maximize the efficiency. This research aims to improve the aerodynamic performance for various ranges of operation wind speed using trailing-edge flap. An optimum blade shape was taken to construct the turbine geometry. The computational model was constructed by ANSYS FLUENT and the k-ω SST turbulence model was used. The computational domain was solved for optimum blade shape with and without trailing edge flap. A various flap deflections were studied for different wind speed and constant rotational speed. The results show that at certain wind speed the turbine performance characteristics were enhancement with increasing the deflection angle (δ) of flap until reach to the maximum improvement and then start to slightly drop. The optimum flap deflection angle changes according to the wind speed values and the optimum values are 5, 10 and 15 degrees at wind speed of 4, 7 and 10m/s respectively. The percentage improvement in lift force is about of 9%, 17.06%, 42.25% and in lift-to-drag ratio is about of 3%, 5%, 23.7% and in power coefficient of about 4.5% %, 17.5%, 17.7% for each wind speed respectively. This is mainly due to improving the stall characteristics over the blade especially near the tip region.

Keywords Horizontal wind turbine, Wind turbine aerodynamic performance, CFD, Wind turbine power enhancement, Trailing-Edge Flap (TEF).

NOMENCLATURE

Abbreviations

HAWT	Horizontal-Axis Wind Turbine
TEF	Trailing-edge flap
CFD	computational fluid dynamic
MPPT	Maximum Power Point Tracking
BEM	Blade Element Momentum
MRS	Multi-Rotor System
FEA	Finite Element Analysis

Symbols

C_L	Lift coefficient
C_D	Drag coefficient
Cp	Power Coefficient
L	Lift force (N)
D	Drag force (N)
L/D	Lift-to-Drag ratio
φ	Pitch angle (Degree)
θ_T	Twist Angle (Degree)
α	Attack Angle (Degree)
T_N	Thrust force (N)
T_Q	Torque (N.m)
Re	Reynolds number
Ω	Rotational speed (rad/s)
R	Turbine rotor radius (m)
r	Local rotor radius (m)
V	Speed of wind (m/s)
V_{rel}	The relative speed of wind (m/s)
$C_{avg.}$	Average chord length (m)
ρ	The air density (kg/m^3)
λ	Tip Speed Ratio
δ	Flap deflection angle (Degree)

1. Introduction

The technology of power generation from wind has been greatly developed in the recent past decades. Improvement the turbine aerodynamic performance is considered one of the most important aspects to increase the turbine efficiency of transforming the energy available in wind into mechanical and to electric energy [1]. In the recent years, a great development and modifications have been made in turbine blade aerodynamic design and the modified HAWT design can be achieve a relatively high-power coefficient compared to the conventional type. However most existing horizontal turbine were designed with a rated power at definite speed of wind [2, 3]. Beyond this range of wind speed, the rotor blades performance faces dangerous phenomena of early separation and then the efficiency of turbine can fall significantly. The problem of early separations is appeared at the inner part of turbine blade especially towards the root of blade, where the air attack angles are raised because of the constraints of structural, like limited of twist angles, blade chord length. The development is the target of study in large turbines aims to reducing the kWh cost. However, a large-scale wind turbine can inevitably cause increasing in turbine blade size and quality [4]. But the next problems must be solved:

- The large-scale turbines have a high inertia, and the single variable-pitch control can hardly cope with quickly change in the loads of aerodynamic under the conditions of turbulent wind [5].
- Use the control system of variable-pitch can cause failure in the pitch-control devices due to fatigue [6].
- Large-scale turbines have a large impeller and high tower; thus, tower shadow and the wind shear can employ huge negative effects on the turbine operation [7].

The stated problems can be alleviated using turbine blades with trailing-edge flap (TEF). The turbine blade with (TEF) can efficiently enhance the lift coefficient and lift-to-drag ratio of turbine rotor. A movable (TEF) offers an important advantage for enhancing the load distribution over the blade length, thus decreasing the mechanical loads and fluctuations of power caused by wind shear, tower shadow, and turbulent flow. After pioneering works of Liebeck, many study research have been steered to clarify the induced phenomena by this device [6]. Recently, more research objects were concentrated on the airfoil section attached several flap profiles, such as Gurney Flap [8, 9], Triangular Flap [10], Trailing-Edge Flaps [11, 12], and deformable Trailing-Edge Flap [13, 14]. The computational simulations were used to investigate the aerodynamic behaviours of (TEF) designed using S809 airfoil section at attack angle range from -5° to 12.5°, the obtained results explain that the lift coefficient and the ratio of lift-to-drag of (TEF) are markedly higher than the conventional flap type and the (TEF) can effectively enhance the stall characteristics at trailing edge of blade [15]. The aerodynamic characteristics of airfoil S809 model with (TEF) with chord length about 10% was investigated numerically for different deflection angles of flap, the results illustrate that the gap between airfoil body and (TEF) has slight effect on air flow characteristics, but the flap deflection has excessive effect on aerodynamic characteristics of airfoil and the greatest lift-to-drag occurs at angle of flap about 14° [16]. The experimental and numerical validation of an offshore turbine airfoils section equipped with an active flap at aft portion of airfoils investigated using CFD and wind tunnel test. This work was performed within a frame of Induflap2-project which partially funded from Danish-funding-board EUDP [17]. The Gurney Flaps effect was predicted using experimental test in Universität Berlin wind tunnel, the tested blade contains two flaps of 1% and 0.5% in heights from chord length, the Gurney Flaps are fixed at trailing-edge and perpendicular to pressure side of blade, the obtained results conclude that, these configurations led to enhancement the turbine performance, attack angles and coefficients of lift due to the certation of wake velocities in axial direction [18]. A comparison of the aeroelastic analysis based on BEM theory against different models such as Free-Wake Lifting Line, higher fidelity, and CFD models were accomplished on oscillating (TEF) of turbine rotor blades to highlight limitations of each model and assesses the main differences between each tools have the same fidelity levels [19]. The effectiveness of Microtabs and trailing-edge flaps have investigation numerically using WTSim, the effects of these control devices of various lengths at several locations on the air flow characteristics of turbine rotor blade are predicted and the power control and enhancement are calculated to ensure where these added devices can be used, it is concluded that the blades combined with (TEF) can rise the turbine power and decrease the turbine blade loading but using the Microtabs has fewer effective in the turbine power production and control [20]. The aerodynamic effects of Gurney flaps combined with vortex generators was study using experimental test in Universität Berlin wind tunnel, the performance of blade was simulated for two cases of flow control devices (without and with the add-ons) and compared between them, it is concluded that the efficiency of aerodynamic is partly improved and the stall is delayed leading to enhancement the turbine power characteristic curve [21]. The comparasion of several researches and studies of the hybrid systems and MPPT methods of the renewable energy resources are explained and review [22]. The conversion systems of wind energy was assessined based on the developed emulator wind wurbine [23]. The benefit and technical solution for the renewable energy resources integration was investigated using the operation concept of the smart grid [24]. The power curve is modelled to monitoring the wind turbine behaviour and operation characteristics [25]. The several researches of conversion systems of wind energy resources and the advantages of using these resources in the smart grids are described and review [26, 27].The aerodynamic performance characteristics of the three MRS wind turbines configurations are calculated and studied using BEM code and the obtained results are compared with the NREL 5MW wind turbine [28].

In the view of above discussion, this work aims to examine the aerodynamic characteristics of (HAWT) equipped with (TEF) to predict the potential benefits of this modification systems on turbine power improvement and to discover the possibility of expending these systems as a

controlling device for power augmentation and load regulation. In this paper, a various flap deflections were studied for different wind speed and constant rotational speed. The effect of (TEF) on turbine rotor blade characteristics were investigated. The turbine rotor power coefficient (Cp), lift (L), drag (D), lift-to-drag ratio (L/D), velocity and pressure contours were predicted. The percentage improvement in power coefficient (Cp), lift (L), drag (D), lift-to-drag ratio (L/D) were determined and discussed, and the stall behaviour were monitored.

2. Numerical Modelling

The process of experimental testing is surely costed and quite laborious. Recently the computational simulations have become a significant tool for optimizing, developing, and validating procedures. In this work, an optimum (OPT) blade shape was taken to generate the turbine geometry of the case study. The turbine blade has three blades of radius about 0.36m with rated power of 50W. The blade shape was designed from NACA-4418 airfoil sections, and the flap at blade trailing-edge is installed from blade middle radius to turbine tip. The flap length about 40% of radius with chord of about 30% from blade chord length. The computational model was constructed by using ANSYS FLUENT and the turbulence were modelled using k-ω SST model of turbulence. The computational simulation was done on three stages as presented in Fig.1 [29]. Firstly, the domain geometry and grid were generated by design modular (DM) of ANSYS program in pre-processing stage. Secondly, the computational domain was solved using ANSYS FLUENT software. The aerodynamic parameters of HAWT blade without and with flap were examined in post-processing stage. The power coefficient (Cp), lift (L), drag (D), lift-to-drag ratio (L/D), contours of pressure, velocity, 3D streamlines, and velocity vectors were illustrated.

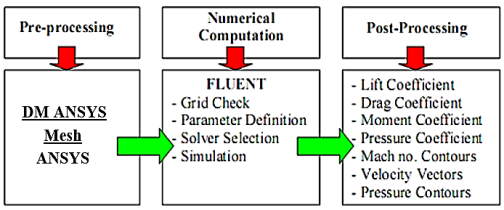

Fig. 1. The three stages of the current CFD modelling [29].

2.1. Blade Shape Geometry and Operation Condition

In this research, an optimum (OPT) blade shape of horizontal-axis turbine without trailing-edge flap (TEF) was selected. This blade has been investigated using both numerically and experimentally for three different geometries of blade with 0.72 m in diameter and NACA-4418 profile [30]. Also, this optimum (OPT) shape of turbine blade, obtained using enhanced (BEM) theory for verifications with the CFD solution. The three blades rotor have a rated power of 50W, and the blade shape was twisted and tapered. The radius, cord, and twist angle of ten sections against the radial direction of turbine blade are summarized and plotted as shown in Table 1. and Fig.2 respectively. The blade twist angles and the chord distribution against the radial direction are plotted in Fig.2a and Fig.2b. Where R: is the total blade radius, r: is the local radius at different section along the blade length, and c: is the local chord at different section along the blade length. All parameters of design which used to calculate the shape of optimal blade by the enhanced (BEM) theory are brief in Table 2. [30].

All forces and angles acting on turbine airfoil section are presented in Fig.3. From this figure, it is easy to get the variation of relative wind angles (φ) as function of pitch (θ_P), twist (θ_T) and attack (α) angles at any airfoil blade sections by using theory of BEM [1, 29, and 30]. Both thrust (T_N) and torque (T_Q) were created by drag (D) and lift (L) forces. Drag and lift forces were obtained using attack angle, Reynolds number (Re), and speed ratio at tip. The (Re) and ratio of tip speed were defined using the following relation as shown in Eq. (1) and Eq. (2):

$$\lambda = (\omega * R) / V \quad (1)$$

$$R_e = (\rho * V_{rel} * C_{avr}) / \mu \quad (2)$$

Where (ω): defined the turbine rotor speed of rotational; (R): defined the radius of turbine; (V): is wind speed; ($C_{avg.}$): defined the mean length of chord for each blade sections; (ρ): defined the density of air; (μ): defined the viscosity of air, and ($V_{rel.}$): defined the speed of relative wind. The coefficient of power (Cp) of turbine blade was defined using Eq. (3):

$$Cp = P_{out} / (0.5\ \rho\ V^3\ \pi\ R^2) = (T_Q \times \omega) / (0.5\ \rho\ V^3\ \pi\ R^2) \quad (3)$$

Table 1. Twist and Chord angle distribution of the OPT shape of blade, [30].

r/R	r (m)	c (m)	Twist angles (deg.)
0.17	0.0612	0.096	25.92
0.26	0.0936	0.085	17.56
0.35	0.126	0.072	12.2
0.44	0.1584	0.061	8.61
0.54	0.1944	0.053	6.08
0.63	0.2268	0.046	4.21
0.72	0.2592	0.041	2.78
0.81	0.2916	0.036	1.65
0.91	0.3276	0.033	0.75
1	0.36	0.03	0

Table 2. Parameters of design for OPT shape of blade, [30].

Turbine Parameters	Value
Rated-Power	50W
Rated-Speed	10m/s
Tip-Speed ratio	5
Turbine blade number	3
Attack angle in (deg.)	5.5
Airfoil section type	NACA-4418

2.2. Computational Domain

A reasonable approximation for HAWT blade model is in avoid the tower, ground, and the rotor hub form the computational solution domain. All computational domain details and dimensions are presented in Fig.4. For simplify the computational solution and time saving, also exploiting the 120° periodicity for the three-blades, a computational

domain has been taken as a sector of cylindrical shape as shown in Fig.4b. A computational domain inlet and outlet have a radius approximately of five and ten times from the turbine blade radius (5R, 10R) respectively measured from the axial centre as shown in Fig.4a. The boundary at inlet has been located at distance equal to five times from the turbine blade radius (5R) upstream of the rotor plane, and the outlet boundary has been located at distance equal to ten times from the turbine blade radius (10R) downstream of rotor plane as shown in Fig.4a.

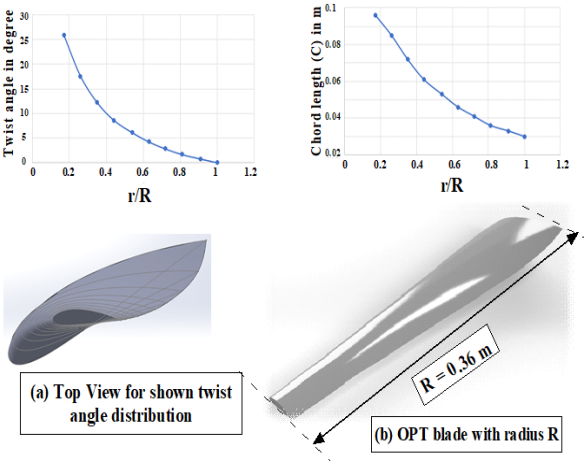

Fig. 2. Parameters of design for OPT shape of a HAWT.

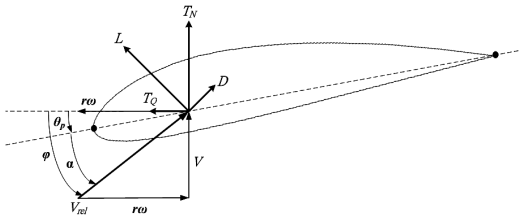

Fig. 3. Diagram of forces and angles acting a section of turbine blade.

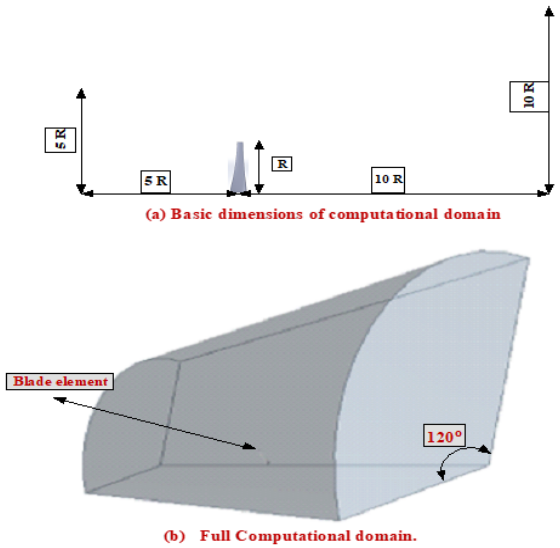

Fig. 4. Main geometry of computational domain of solution.

2.3. Boundary Conditions

A numerical model of NACA-4418 turbine blades were solved using FLUENT ANSYS. A flow field, temperature, pressure, velocity, and all aerodynamic characteristics were predicted using the following boundary conditions as presented in Fig.5. The boundary of inlet and the upper face of cylinder are assumed to a uniform flow with a speed of about 10m/s and the attack angle of 5.5 degree. The two side walls are assumed as a periodic boundary (Rotational type). The blade faces are assumed as a wall with condition of no-slip, and finally the face outlet assumed as a pressure outlet. The temperature of free stream is the environmental temperature of a value about 288.16 K. The main property of air flow such as density, pressure, and viscosity at the given temperature are 1.225kg/m^3, 101325Pa and 1.7894×10^{-5}kg/m respectively. The interiors of computational domain were rotated in the negative y-direction with same speed of rotational of rotor blades (ω).

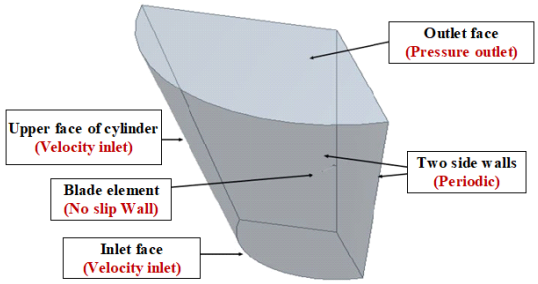

Fig. 5. The operation boundary conditions of the Computational domain.

2.4. Mesh Generation

To obtain accurately results, the grids near the rotor blade walls was dense enough and computed domain was large enough as possible to balance the accuracy versus solution time of calculation. However, excessive grids and field dimensions will be cost too much calculating and slowing the computing speed. Also using unstructured tetrahedral grid mesh for overall domain increasing the number of cells in solution domain, it is required supercomputer and extra time to solve. Several studies developed different methods and tools to vanish these described problems in this research. [32] presented several methods of grid generation to create high quality multi-block grid structure that used for complex shape. In this work, the multi-block grid method was used to improve grids near rotor blade volume with creating sphere near the blade volume and making body inflation. It is created face inflation and face sizing in 3D blade volume faces which reduce the computational time and obtain accurate aerodynamic characteristics of the turbine rotor. The mesh was generated and adapted using ANSYS FLUENT MESH as presented in Fig.6. To adapt a little grid size of boundary layers at blade walls, the method of body sizing was used for a sphere near the blade volume also the certain growth rate was increased to a maximum the grid size far away the main boundary. The applied body sizing has minimum size of element of about 2.9827×10^{-5}m at blade walls and its procedures a growth rate of 1.05 and a maximum size of element of about 0.2m. The used type of grid is tetrahedral-hybrid unstructured grids with quality of domain meshing of 0.23371 average skewness which a good value for quality of mesh. Finally, the total cells number is about 2500000 cells.

2.5. Grid dependency check

Study the independency of grids were performed to reduce the grid cells number without failing accuracy. Generally, the computational simulation becomes extra accurate for used additional cells, but using extra cells increases the needed time and computer memory. The suitable number of nodes are determined using growing the cells number up to the grid is sufficiently refine so, additional refinement does not affect the results. To determine the independence of results to cells number, twelve types of grid mesh were generated. Fig.7 shows grid cells number effect on the power coefficient of turbine at wind velocity inlet 10 m/s with optimum attack angle of 5.5 degree and speed of rotational 136.67 rad/sec at design ratio of the tip speed is 4.92. All results were done using an intel computer of core-i7 with 16GB RAM and convergence criteria was setting to decrease the solution residual scale (the absolute error value between each iteration and the next one) under value of about 10^{-5}. For reducing the time of solution without failing accuracy, the mesh that has 2500000 cells was taken as presented in Fig.(7).

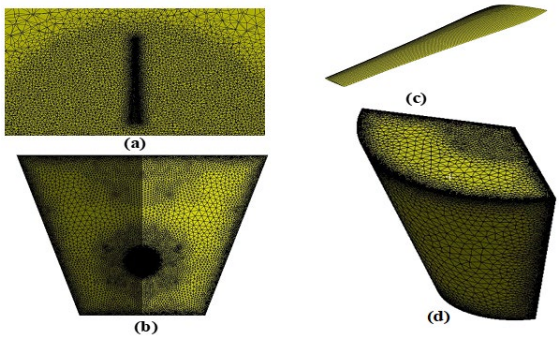

Fig. 6. Meshing of Computational domain of 3D blade volume (a) Section view shown inflation around blade (b) Lower view for Computational domain (c) Blade Meshing surface (d) Isometric of Computational domain.

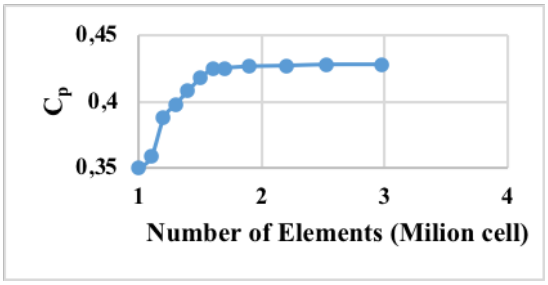

Fig. 7. Power coefficient against grid cells number at wind velocity 10 m/s.

2.6. Numerical Model Verification

To validate the computational solution of the OPT turbine blade with NACA-4418 sections, the numerical model of the case study was compared with an experiment, numerical and BEM theory model which studied with same operation conditions [31]. From previous CFD of turbine research, the model of k-ω SST was used for turbulence [2, 10, 16, 30, and 31]. The parameters of simulation of the case study been adjusted with the same operation conditions of compared cases. The computational results illustrate a good match of the coefficient of power with the consistent values of experimental, numerical, and BEM theory [30], with a maximum error of about 0.1% from experimental measurements as presented in Fig.8.

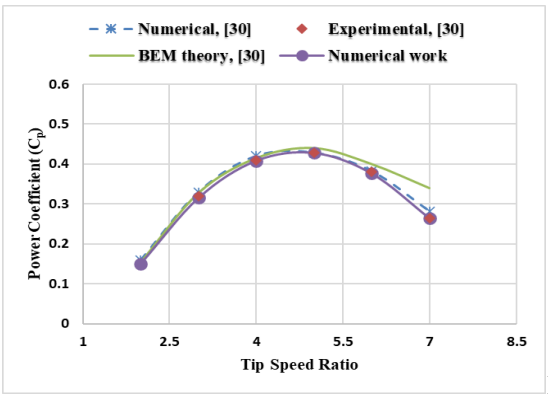

Fig. 8. Turbine power coefficient against tip-speed ratio.

3. Turbine Blade with Flap (TEF)

Enhancing aerodynamic characteristics of wind turbine rotor is considered a significant factor to increase the converting efficiency of kinetic energy available from wind to mechanical and then to electrical. In this research, effect of (TEF) deflection (δ) on HAWT aerodynamic characteristics were examined at varies wind velocity. An optimum blade shape (OPT) turbine rotor was taken to build the turbine geometry of the case study. The turbine rotor has three blades of radius about 0.36 m with power rated of about 50W. The shape of blade was designed from NACA-4418 airfoil blade sections. The trailing-edge flap is installed from blade middle radius to tip. The length of flap is 40% of blade radius with length of chord 30% from the length of blade chord. The main geometry parameters of turbine rotor with (TEF) were illustrated in Fig.9. To examine the trailing-edge flap effect on the improvement of turbine performance, the constructed computational domain was solved using ANSYS FLUENT for (OPT) turbine blade without and with flap. The mesh was generated using ANSYS FLUENT MESH as presented in Fig.10. The type of grid is tetrahedral-hybrid unstructured grid with quality of domain meshing of 0.23371 average skewness which a good value for quality of mesh. Finally, the overall number on cells in domain is about 2500000 cells. A different flap deflection was studied at various speed of wind and constant rotational speed of about 136.67 rad/sec. The speed of wind is 4, 7, and 10m/s with a ratio of tip speed (λ) about 12.3, 7.03 and 4.92. The flap deflections were studied at four deflection angles (δ) of 5, 10, 15 and 20 degrees.

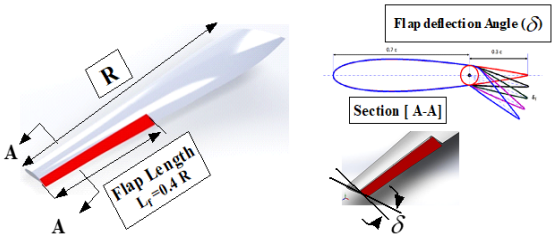

Fig. 9. Turbine blade with TEF parameters.

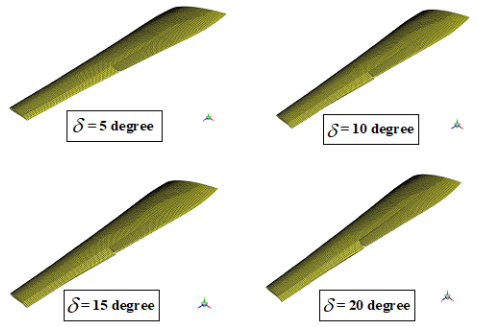

Fig. 10. OPT blade meshing with varies deflection angles.

4. Result and Discussions

To investigate the flap effect on enhancement of turbine performance, the solution domain was solved using ANSYS FLUENT for (OPT) turbine blade without and with flap. A various flap deflections were studied at various operation speed for constant rotational speed of about 136.67 rad/sec. The speed of wind is 4, 7, and 10m/s with the ratio of tip speed (λ) of about 12.3, 7.03 and 4.92. The deflection of flap was examined at deflection angles (δ) of 5, 10, 15 and 20 degrees. The pressure contours, velocity contours, lift (L), drag (D), lift-to-drag ratio (L/D), and coefficient of power (C_P) were predicted for (OPT) turbine blade without and with flap and then compared between them to calculate the percentage improvement.

4.1. Turbine Rotor Blade Without Trailing-Edge Flap (TEF)

4.1.1. Velocity Vector and Velocity Contours

The velocity vectors of (OPT) blades without TEF at operation speed of about 10m/s and design ratio of the tip speed of about 4.92 are presented in Fig.11. The velocity contours of (OPT) blades without TEF for various radial sections along turbine blade length were predicted at operation speed of about 10m/s and design ratio of the tip speed of 4.92 as shown in Fig.12. These radial sections are [r/R = 0.5, 0.75, 0.93, 0.95, 0.97 and 0.99]. From figure it is noted that, velocity of upper surface is greater than lower surface for all radial sections along the turbine radius. The different in velocity magnitude between upper and lower surface increase from root to tip sections. The separations of flow near the trailing edge of blade were decreased from root to tip sections, that's indicated maximum lift force and minimum drag force.

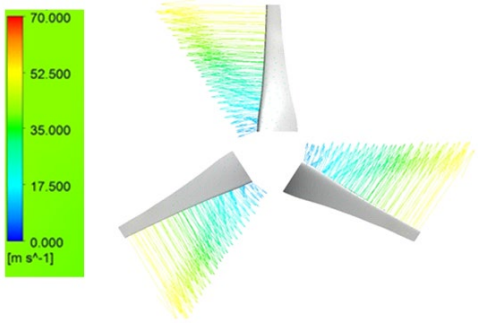

Fig. 11. Velocity vectors around (OPT) turbine rotor blades.

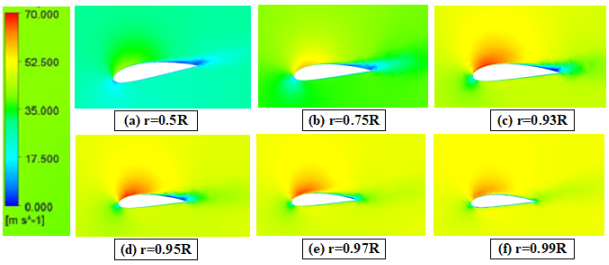

Fig. 12. The velocity contours distributions at various radial sections of (OPT) blades without TEF, at V=10(m/s) and λ=4.92 (Flap deflection angle = 0 degree).

4.1.2. Pressure Contours

The static pressure contours of (OPT) blades without TEF for various radial sections along turbine blade length were predicted at operation speed of about 10m/s and design ratio of the tip speed 4.92 as shown in Fig.13. These radial sections are [r/R = 0.5, 0.75, 0.93, 0.95, 0.97 and 0.99]. From figure it is noted that, static pressure of lower surface is greater than upper surface for all radial sections along the turbine radius. The difference in static pressure between lower and upper surface increase from root to tip sections. The tangential forces and lift increase from root to tip, this leads to rise the turbine power generation.

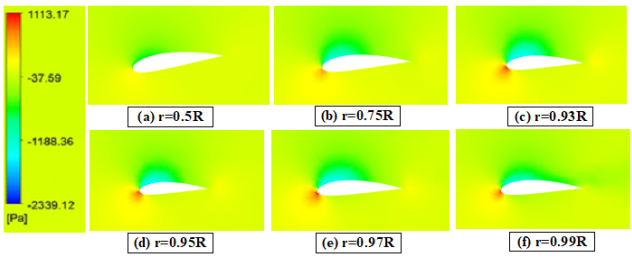

Fig. 13. The distributions of static pressure contours at various radial sections for (OPT) blade sections without TEF, at V=10(m/s) and λ=4.92 (Flap deflection angle = 0 degree).

4.2. Turbine Rotor Blade with Trailing-Edge Flap (TEF)

4.2.1. Velocity contours

The velocity contours of (OPT) blades with TEF for different radial sections along the turbine radius were predicted at operation speed of about 10m/s and design ratio of the tip speed of about 4.92 as present in Fig.14. These radial sections are [r/R = 0.5, 0.75, 0.93, 0.95, 0.97 and 0.99] and the presented flap deflection angles are 10, 15 and 20 degrees. The calculated results are compared with the corresponding results of (OPT) blades without TEF (zero flap deflection, Fig.12). In general, it is noticing the deflection of flap increase the flow velocity on entire upper surface of turbine blade sections also decrease the velocity of flow close to the airfoil trailing edge of lower surface. All velocity contours for flap deflection of 10 degree are presented in Fig.14a. From figure it can note that, the velocity in lower surface decreases (blue area increasing) and the velocity in upper surface increases (red area increasing) than the blade without TEF that's indicated growth in the turbine rotor lift force. The velocity contours for flap

deflection of 15 degree are presented in Fig.14b. The velocity in lower surface is still decrease and the velocity in upper surface is still increase that's indicated growth in turbine rotor lift force. The velocity contours for flap deflection of 20 degree are presented in Fig.14c. The velocity in lower surface is still decrease (blue area increasing than flap deflections of 10 and 15 degree on lower surface) but the velocity in upper surface is decreasing than other cases of the turbine flap deflection (red area decreasing than flap deflections of 10 and 15 degree on lower surface). These flow behaviour leads to decrease in lift and increase in drag forces. At certain wind velocity, it is noting as the deflection of flap increases, the turbine aerodynamic characteristics improves until certain flap deflection angle and then the turbine characteristics declines. Finally, it can accomplish that, the variation in flow pressure due to flap defections leads to growth in the turbine rotor lift force and improve the turbine characteristics and then increase the power of turbine. This is mainly due to enhancement in the characteristics of stall at the turbine blade trailing-edge.

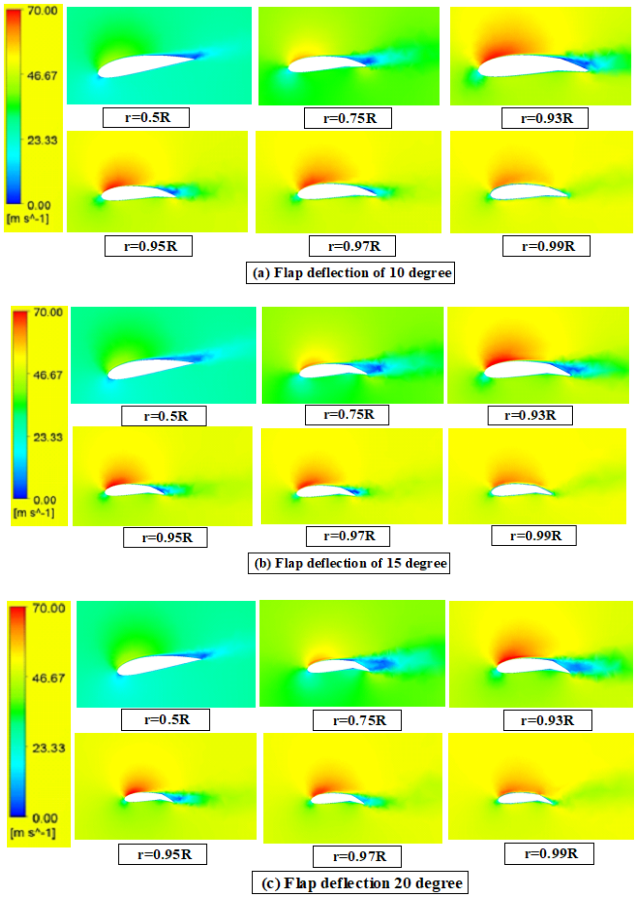

Fig. 14. The velocity contours distributions at various radial sections for (OPT) blade sections with TEF, for V=10(m/s), λ=4.92, different flap deflections of 10, 15, and 20 degrees.

4.2.2. Pressure contours

The contours of static pressure of OPT turbine blades with TEF for various radial sections along the turbine blade length were predicted at operation speed of 10m/s and design ratio of the tip speed 4.92 as displayed in Fig.15. These radial sections are [r/R = 0.5, 0.75, 0.93, 0.95, 0.97 and 0.99] and the presented flap deflection angles are 10, 15 and 20 degrees. The calculated results and the corresponding results of OPT turbine blades without TEF (zero flap deflection, Fig.13) are compared with each other. In general, it is note that the deflection of flap decreases the pressure on the entire upper suction surface of blade airfoil and raises the pressure on a lower airfoil surface nearby the blade trailing-edge of turbine. The variation of pressure contours for flap deflection of 10 degree are presented in Fig.15a. From figure it can show that, the lower surface pressure was increases (red area increasing) and the upper surface pressure was decreases (blue area increasing) than the turbine blade without TEF that's indicated increase in the turbine rotor lift force. The pressure contours for flap deflection of 15 degree are presented in Fig.15b. The lower surface pressure is still increases and the pressure of upper surface is still reducing that's indicated growth in the turbine rotor lift force. The pressure contours for flap deflection of 20 degree are presented in Fig.15c. The lower surface pressure is still increase (red area increasing than flap deflections of 10 and 15degree on lower surface) but the upper surface pressure is increase than other cases of flap deflection (blue area decreasing than flap deflections of 10 and 15 degree on lower surface). These flow behaviour leads to decrease the turbine rotor lift force also increase the drag force. At certain wind velocity, it is noting as the flap deflection increases, the turbine aerodynamic characteristics improves until certain flap deflection angle and then the turbine characteristics declines. Finally, it can note, the variation in flow pressure due to flap defections leads to increase the turbine rotor lift force and improve the turbine characteristics and then increase the power of turbine. This is mainly because of enhancement the stall characteristics of the turbine blade trailing-edge.

4.2.3. The turbine rotor Lift and Drag Forces

The rotor lift of (OPT) turbine blades with TEF for different flap deflection angles and different wind speed are investigated at constant speed of rotational 136.67 rad/sec as illustrated in Fig.16. The studied deflection angles of flap are 5, 10, 15 and 20 degrees for speed of wind 4, 7 and 10m/s with the ratio of tip-speed (λ) of about 12.3, 7.03 and 4.92. The calculated results and the corresponding results of OPT turbine blades without TEF (zero flap deflection) are compared with each other. From Fig.16 in general for all operation wind speed it is note, the rotor lift force increasing with increasing flap deflection angle until reach to optimum value and then decreases. Also, from result we can note that the optimum value of lift force and corresponding flap deflection angle change related to the operation wind speed value. At speed of (v=4m/s), the optimum flap deflection angle is about 5 degrees with improving in lift force by about 9% from zero flap deflection. At speed (v=7m/s), the optimum flap deflection angle is about 10 degrees with improving in lift force by about of 17.06% from zero flap deflection. For speed v=10 m/s, the optimum flap deflection angle is about 15 degrees with improving in lift force by about 42.25% from zero flap deflection. The lift force was enhanced because improving in the turbine stall characteristics. The dash red line in Fig.16 was illustrate the

maximum value of lift force against the optimum value of flap deflection angle for different operation wind speed. The drag force of (OPT) turbine blades with TEF for different flap deflection angles and various operation speed were investigated at constant speed of rotational 136.67 rad/sec as presented in Fig.17. From this figure it is note, in general the drag force increasing with increasing flap deflection angle for all operation wind speed of turbine rotor.

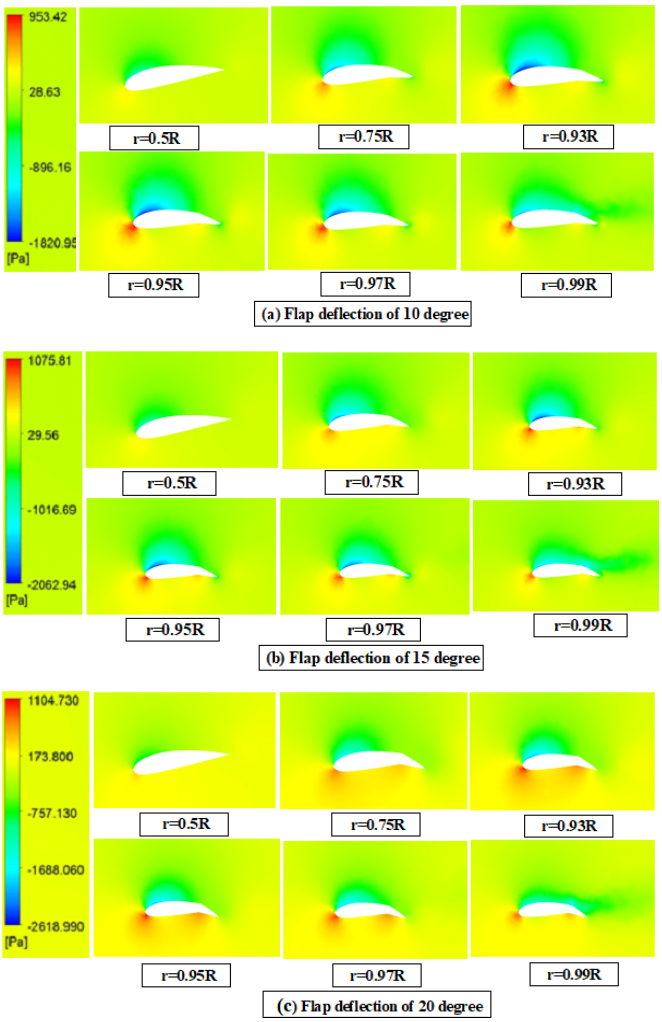

Fig. 15. The static pressure contours distributions at various radial sections for OPT blades with TEF, for V=10(m/s), λ=4.92, different flap deflections of 10, 15, and 20 degrees.

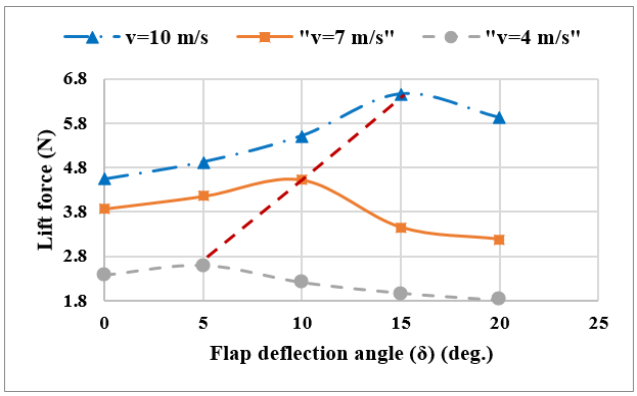

Fig. 16. The lift force for OPT blade against flap deflection angle at various operation speed.

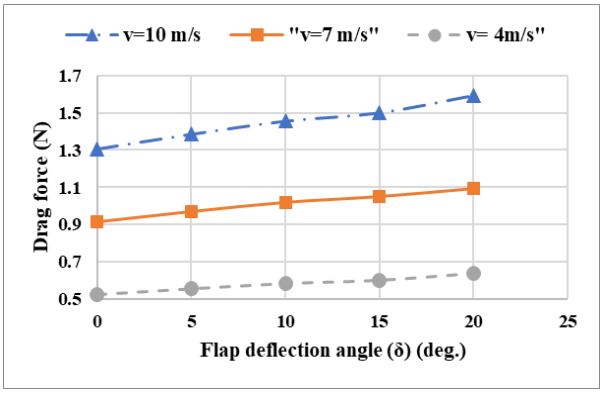

Fig. 17. The drag force for OPT blade against flap deflection angle at various operation speed.

4.2.4. The Ratio of Lift to Drag (L/D)

The ratio lift coefficient to drag coefficient (C_L/C_D) of OPT blades with TEF for different flap deflection angles and different operation speed were investigated at constant speed of rotational 136.67 rad/sec as presented in Fig.18. From this figure it is noting, the ratio of lift-to-drag has been increasing with increasing flap deflection angle until reach to optimum value and then decreases. Also, from result we can note the optimum quantity of the ratio of lift related to drag and corresponding flap deflection angle change related to the operation speed value. The coefficient of (C_L/C_D) was improving from zero deflection of flap by about of 3%, 5%, and 23.7% for wind speed v=4m/s, v=7m/s, v=10m/s respectively. This improving in (C_L/C_D) have great effect in efficiency of the turbine, [1, 24].

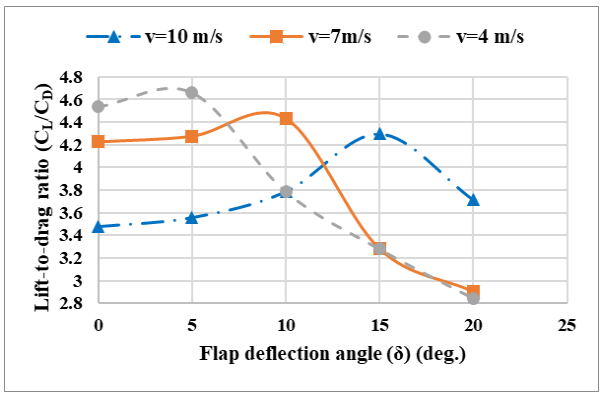

Fig. 18. The (L/D) ratio for OPT blade against flap deflection angle at various operation speed.

4.2.5. Power coefficient (Cp)

The coefficient of power (C_P) of (OPT) turbine blades with TEF for different flap deflection angles and various operation speed were investigated at constant speed of rotational 136.67 rad/sec as presented in Fig.19. From this figure it is noting, the coefficient of power (C_P) increasing with increasing flap deflection angle until reach to optimum value and then this ratio decreasing. Also, from result we can see that the optimum value of the coefficient of turbine power (C_P) and corresponding flap deflection angle change according to wind speed value. The coefficient of turbine power was improving from zero deflection of flap by about

4.5%, 17.7%, and 17.5% for wind speed v=4m/s, v=7m/s, v=10m/s respectively.

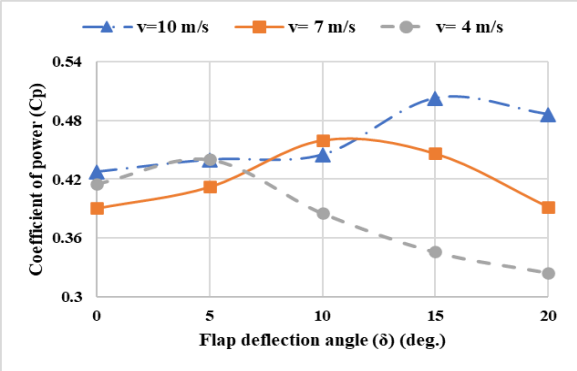

Fig. 19. The coefficient of power (Cp) for OPT blade with TEF deflection angle at various operation speed.

4.2.6. *Effect of the flap angle of deflection on flow behaviours*

For understanding the effect of flap deflection angle on turbine characteristics, the streamline flow distribution over three sections along the turbine blade length are predicted at various flap angles as presented in Fig.20, Fig.21, Fig.22, and Fig.23 respectively. In general, these figures show the dangerous effect of vortex on turbine performance. Also, the vortex strength increases at plane section of (r/R) = 75% especially at flap deflection angels of 20° and 25° as seen in Fig.22c, and Fig.23c respectively. In contrast, the strength of vortex does not appear at flap deflection angels of 10° and 15° at plane section of (r/R) = 50% and (r/R) = 75% and start to grow at flap deflection angels of 20° and 25° as presented in Fig.22a, Fig.22b, and Fig.23a, Fig.23b respectively. Finally, the high strength of flow vortex dose appears at flap deflection angels of 20° and 25° at plane of (r/R) = 75% as presented in Fig.22, and Fig.23 respectively.

4.2.7. *Effect of the flap angle of deflection on the distributions of pressure coefficient*

To understanding the angle of deflection effect on the turbine performance, the distribution of coefficient of pressure along dimensionless (x/c) cord ratio are studied over three sections along the blade length at various flap angles as presented in Fig.24, Fig.25, and Fig.26 respectively. In general, these figure shows that an improvement in coefficient of pressure because of the deflection of flap. At plane of (r/R)=50% the enhancement in pressure coefficient distribution has little value for all flap deflection value as presented in Fig.24. At plane of (r/R)=75% and (r/R)=97% the improvement ratio in pressure coefficient distribution value is increased for all value of flap deflection as presented in Fig.25 and Fig.26 respectively. This improvement because installed the flap at the outer portion of turbine rotor length.

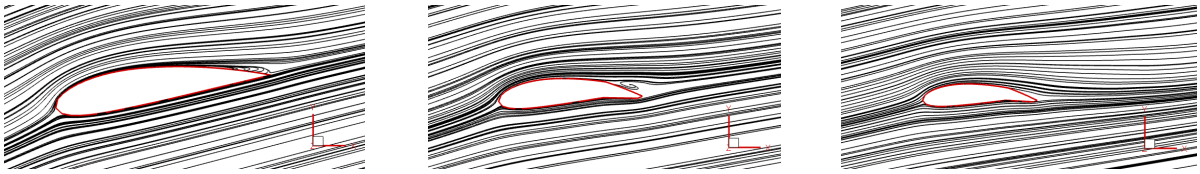

(a) Plane of (r/R = 50%) **(b) Plane of (r/R = 75%)** **(c) Plane of (r/R = 97%)**

Fig. 20. Streamlines behaviours of flow at various radial sections for flap angle of 10 degrees.

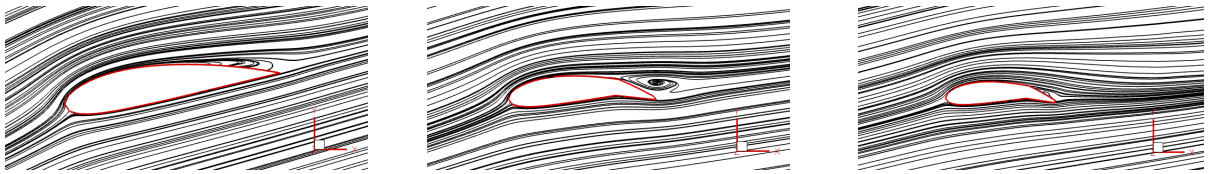

(a) Plane of (r/R = 50%) **(b) Plane of (r/R = 75%)** **(c) Plane of (r/R = 97%)**

Fig. 21. Streamlines behaviours of flow at various radial sections for flap angle of 15 degrees.

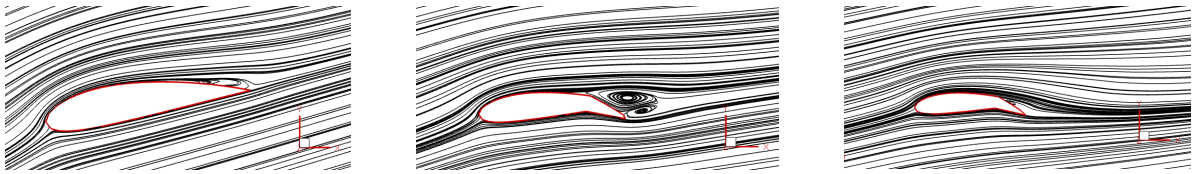

(a) Plane of (r/R = 50%) **(b) Plane of (r/R = 75%)** **(c) Plane of (r/R = 97%)**

Fig. 22. Streamlines behaviours of flow at various radial sections for flap angle of 20 degrees.

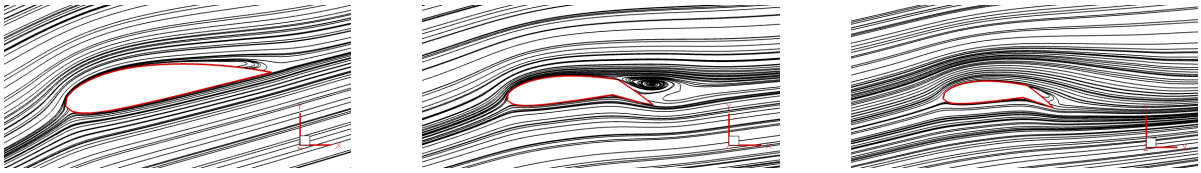

(a) Plane of (r/R = 50%) **(b) Plane of (r/R = 75%)** **(c) Plane of (r/R = 97%)**

Fig. 23. Streamlines behaviours of flow at various radial sections for flap angle of 25 degrees.

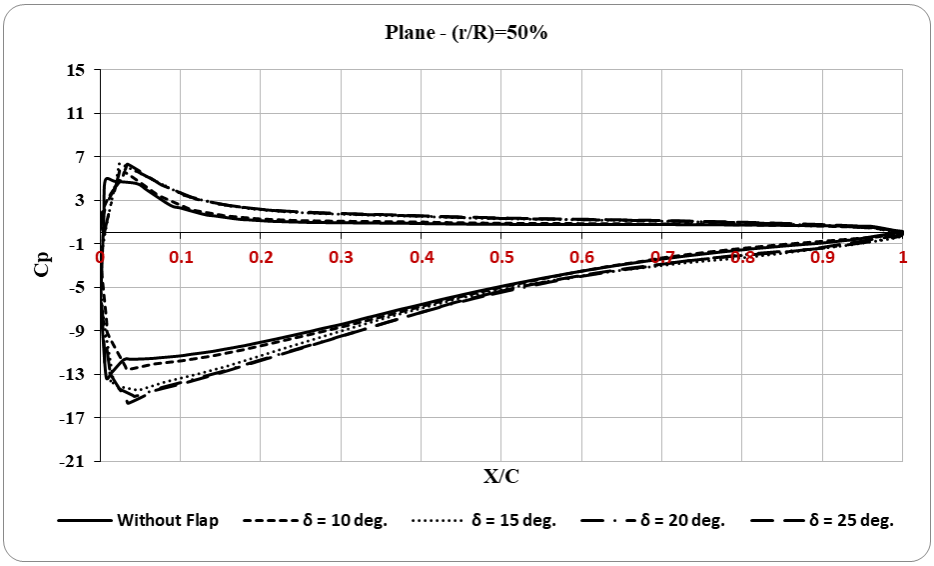

Fig. 24. Pressure coefficient variation at radial sections of (r/R=50%) for different flap angles.

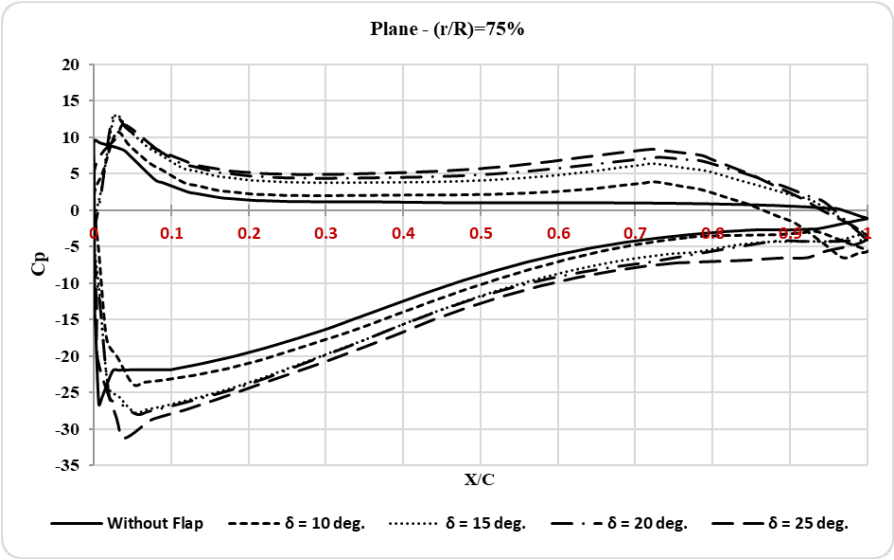

Fig. 25. Pressure coefficient variation at radial sections of (r/R=75%) for different flap angles.

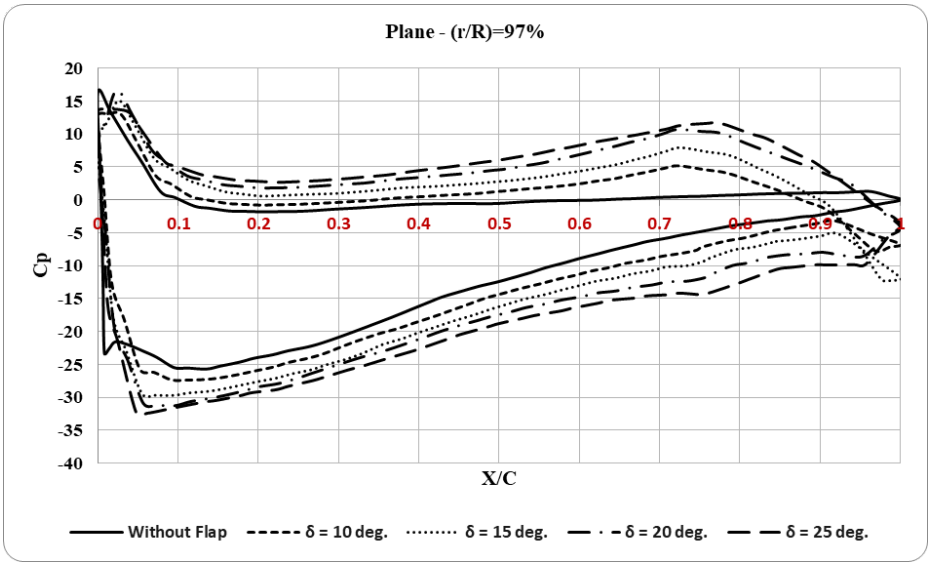

Fig. 26. Pressure coefficient variation at radial sections of (r/R=97%) for different flap angles.

5. Conclusion

In this work, an optimum wind turbine blade shape (OPT) was taken to construct the turbine geometry of the case under consideration. A trailing-edge flap is installed from blade middle radius to tip. The computational solution domain was solved using ANSYS FLUENT for (OPT) turbine blade shape without and with trailing-edge flap, and the model (k-ω SST) was used for turbulence. The validation results show good agreement by a maximum error of about 0.1%. A various flap deflections were studied at different speed of wind and constant rotational speed of about 136.67 rad/sec. The operation speed of wind is 4, 7, and 10m/s with the ratio of tip speed (λ) of about 12.3, 7.03 and 4.92 respectively. The flap deflections were studied at deflection angles (δ) of 5, 10, 15 and 20 degrees. In general, the obtained results show that at certain operation speed the wind turbine characteristics were enhancement with increasing the deflection angle of flap (δ) until reach to the maximum improvement at optimum angle and then start to slightly drop and the optimum flap deflection angle varies related to the operation speed value. From the obtained results noting that the optimum flap deflection angle (δ) are 5, 10 and 15 degrees at operation speed of 4, 7 and 10m/s respectively. The percentage enhancement in the turbine rotor lift force, lift-to-drag ratio and power coefficient are about 9%, 3%, 4.5% and 17.06%, 5%, 17.5% and 42.25%, 23.7%, 17.7% at operation speed value of 4, 7, and 10m/s respectively. These improvement in the rotor performance characteristics mainly due to improving the stall characteristics over the turbine rotor blade especially near the blade tip. Finally, we can conclude that control the flap deflection angle to optimum value will be offer improvement in the wind turbine characteristics and then enhance the generated turbine power on a large range of operation speed of wind.

Declaration of Conflicts of Interests

Funding: Authors state that this research did not receive any specific grant from funding agencies in the public, commercial, or not-for-profit sectors.

Conflicts of interest/Competing interests: Nil

Availability of data and material: Data files are available upon request

References

[1] M. O. L. Hansen, Aerodynamics of wind turbine, 2nd ed., by Earthscan in the UK and USA, 2008. https://doi.org/10.4324/9781849770408

[2] H. Chen and N. Qin, "Trailing-Edge flow control for wind turbine performance and load control", Renewable Energy, 105. pp. 419-435. ISSN 0960-1481, 2016, https://doi.org/10.1016/j.renene.2016.12.073.

[3] T. K. Barlas, and G. A. M. Van Kuik, "Review of State of The Art In Smart Rotor Control Research For Wind Turbines" Progress in Aerospace Sciences,46(1), 1-27, 2010, https://doi.org/10.1016/j.paerosci.2009.08.002.

[4] H. A. Madsen, "Development of Smart Blade Technology-Trailing Edge Flaps. Roskilde, Danmark: DTU Wind Energy" Annual Report, 2013: 12-13.

[5] L. Bergami, M. Gaunaa, and V. Riziotis, "Aerodynamic Response of An Airfoil Section Undergoing Pitch Motion And Trailing Edge Flap Deflection: A Comparison Of Simulation Methods". Wind Energy, 17(3):389-406,2014.

[6] S. G. Lee, S. J. Park, K. S. Lee, and C. Chung," Performance Prediction of NREL Phase VI Blade Adopting Blunt Trailing Edge Airfoil".Energy, 47(1): 47-61, 2012, https://doi.org/10.1016/j.energy.2012.08.007.

[7] R.H. Liebeck, "Design of subsonic airfoils for high lift." J. Aircr. 547–561, 1978, https://doi.org/10.2514/3.58406.

[8] Y. Amini, H. Emdad, and M. Farid, "Adjoint Shape Optimization of Airfoils With Attached Gurney Flap". Aerosp. Sci. Technol. 41, 216–228, 2015, https://doi.org/10.1016/j.ast.2014.12.023.

[9] H.R. Xu, H. Yang, and C. Liu, "Numerical value analysis on aerodynamic performance of DU series airfoil with thickened trailing edge." Trans. Chin. Soc. Agric. Eng. 30, 101–108, 2014, https://doi.org/10.3969/j.issn.1002-6819.2014.17.014.

[10] V. Yashodhar, G. Humrutha, M. Kaushik, and S.A. Khan, "CFD Studies on Triangular Micro-Vortex Generators in Flow Control." In IOP Conference Series: Materials Science and Engineering; IOP Publishing: Bristol, UK, Volume 184, p. 012007, 2017, https://doi.org/10.1088/1757-899X/184/1/012007.

[11] T. Lee, and Y.Y. Su, "Unsteady Airfoil with A Harmonically Deflected Trailing-Edge Flap", J. Fluids Struct. 27, 1411–1424, 2011, https://doi.org/10.1016/j.jfluidstructs.2011.06.008.

[12] M. Seyednia, M. Masdari, and S. Vakilipour, "The Influence of Oscillating Trailing-Edge Flap On The Dynamic Stall Control Of A Pitching Wind Turbine Airfoil." J. Braz. Soc. Mech. Sci. Eng. 41, 192, 2019, https://doi.org/10.1007/s40430-019-1693-z.

[13] W.S. Lu, Y. Tian, and P.P. Liu, "Aerodynamic optimization and mechanism design of flexible variable camber trailing-edge flap." Chin. J. Aeronaut. 30, 988–1003, 2017, https://doi.org/10.1016/j.cja.2017.03.003.

[14] W.G. Zhang, X.J. Bai, Y.F. Wang, Y. Han, and Hu, Y. "Optimization of Sizing Parameters And Multi-Objective Control Of Trailing Edge Flaps On A Smart Rotor." Renew. Energy, 129, 75–91, 2018. https://doi.org/10.1016/j.renene.2018.05.091.

[15] X. Bofeng, F. Junheng, L. Qing, X. Chang, Z. Zhenzhou, and Y. Yue," Aerodynamic Performance Analysis of a Trailing-Edge Flap for Wind Turbines" Phys.: Conf. Ser. 1037 022020, 2018, https://doi.org/10.1088/1742-6596/1037/2/022020.

[16] Y. L. Jia, Z. H. Han, F. Y. Li, Y. Bai, and J. X. Wang, "influence of flap deflection angle on wind turbine airfoil with trailing edge flaps", Advanced materials Research,

2014,https://doi.org/10.4028/www.scientific.net/AMR.977.222

[17] A. G. Gonzalez, P. B. Enevoldsen, B. Akay, T. K Barlas, A. Fischer, and H. A. Madsen" Experimental and numerical validation of active flaps for wind turbine blades", IOP Conf. Series: Journal of Physics: Conf. Series 1037 (2018) 022039, https://doi.org/10.1088/1742-6596/1037/2/022039.

[18] J. Alber, R. Soto-Valle, M. Manolesos, S. Bartholomay, C. N. Nayeri, M. Schönlau, C. Menzel, C. O. Paschereit, J. Twele, and J. Fortmann" Aerodynamic effects of Gurney flaps on the rotor blades of a research wind turbine", Wind Energ. Sci., 5, 1645–1662, 2020, https://doi.org/10.5194/wes-5-1645-2020.

[19] J. M. Prospathopoulos, V. A. Riziotis, E. Schwarz, T. Barlas, M. Aparicio-Sanchez, G. Papadakis, D. Manolas, G. Pirrung, and T. Lutz, " Simulation of oscillating trailing edge flaps on wind turbine blades using ranging fidelity tools", Wind Energy, 24(4), 357-378, 2021, https://doi.org/10.1002/we.2578.

[20] A. Maheri, I. K. Wiratama, and T. Macquart, " Performance of Microtabs and Trailing Edge Flaps in Wind Turbine Power Regulation: A Numerical Analysis Using WTSim", JREE: Vol. 9, No. 2, 18-26, Spring 2022, https://doi.org/10.30501/JREE.2021.291397.1220.

[21] J. Alber, M. Manolesos, G. Weinzierl-Dlugosch, J. Fischer, A. Schönmeier, C. N. Nayeri, C. O. Paschereit, J. Twele, J. Fortmann, P. F. Melani, and A. Bianchini," Experimental investigation of mini-Gurney flaps in combination with vortex generators for improved wind turbine blade performance", Wind Energ. Sci., 943–965, 2022, https://doi.org/10.5194/wes-7-943-2022.

[22] R. Z. Caglayan, K. Kayisli, N. Zhakiyev, A. Harrouz, and I. Colak, "A Review of Hybrid Renewable Energy Systems and MPPT Methods" International journal of smart grid, Vol.6, No.3, 72–82, September 2022. https://doi.org/10.20508/ijsmartgrid.v6i3.248.g196

[23] Y. Elsayed, N. H. Saad, and A. Zekry "Assessing Wind Energy Conversion Systems Based on Newly Developed Wind Turbine Emulator" International journal of smart grid, Vol.4, No.4, 139-148, December, 2020. https://doi.org/10.20508/ijsmartgrid.v4i4.133.g101

[24] K. E. Ouedraogo, P. O. Ekim, and E. Demirok, "Decimal States Smart Grid Operations Concept: Technical Solution and Benefit for Renewable Energy Integration", 11th International Conference on Renewable Energy Research and Applications, (ICRERA 2022).

[25] R. J. d. A. Vieira, and M. A. Sanz-Bobi, "Power curve modelling of a wind turbine for monitoring its behaviour", 4th International Conference on Renewable Energy Research and Applications, (ICRERA 2015). https://doi.org/10.1109/ICRERA.2015.7418571

[26] O. ALKUL, D. Syed, and S. Demirbas "A Review of Wind Energy Conversion Systems", 10th IEEE International Conference on Smart Grid, (icSmartGrid 2022). https://doi.org/10.1109/icSmartGrid55722.2022.9848755

[27] M. Cakir, I. Cankaya, I. Garip, and I.Colak "Advantages of Using Renewable Energy Sources in Smart Grids", 10th IEEE International Conference on Smart Grid, (icSmartGrid 2022). https://doi.org/10.1109/icSmartGrid55722.2022.9848612

[28] A. Elkodama, A. Ismaiel, A. Abdellatif, and S. Shaaban "Aerodynamic Performance and Structural Design of 5 MW Multi Rotor System (MRS) Wind Turbines" International journal of renewable energy research, Vol.12, No.3, 1495–1505, September 2022. https://doi.org/10.20508/ijrer.v12i3.13343.g8535

[29] E. S. Abdelghany, E. E. Khalil, O. E. Abdelatif, and G. M. ElHarriry, "Computational analyses of aerodynamic characteristics of naca653218airfoil", Proceedings, AIAA paper AIAA_2016_1_ 2307246.

[30] F. B. Hsiao, C. J. Bai, and W. T. Chong, " the performance test of three different horizontal axis wind turbine (hawt) blade shapes using experimental and numerical methods", Energies 6, 2784-2803, 2013, https://doi.org/10.3390/en6062784.

[31] C.J.Bai, F.B.Hsiao, M.H.Li, G.Y.Huang, and Y.J.Chen, "code development for predicting the aerodynamic performance of a hawt blade with variable-operation and verification by numerical simulation", proceedings for 17th National CFD Conference, Taoyuan, Taiwan, 29–31, July 2010, https://doi.org/10.1016/j.proeng.2013.12.027.

[32] E. S. AbdelGhany, " cfd investigation for effect of the aerodynamic truck-cabin profiles and devices on the truck performance", IJMME-IJENS, ID: 200903-6868, Pages: 1-17 , June, 2020.